

5

Copy  
RM L55E16a

CONFIDENTIAL



3 1176 00084 1172



# RESEARCH MEMORANDUM

A DISCUSSION OF RECENT WIND-TUNNEL STUDIES RELATING  
TO THE PROBLEM OF ESTIMATING VERTICAL- AND  
HORIZONTAL-TAIL LOADS

By Richard E. Kuhn, Joseph M. Hallissy, Jr.,  
and Ralph W. Stone, Jr.

Langley Aeronautical Laboratory  
Langley Field, Va.

CLASSIFICATION

UNCLASSIFIED

To \_\_\_\_\_

*DNCA Res dir*

*VRN-127*

*effective*

Date *May 16, 1958*

By authority of \_\_\_\_\_

*AMTG-16-58*

CLASSIFIED DOCUMENT

This material contains information affecting the National Defense of the United States within the meaning of the espionage laws, Title 18, U.S.C., Secs. 793 and 794, the transmission or revelation of which in any manner to an unauthorized person is prohibited by law.

## NATIONAL ADVISORY COMMITTEE FOR AERONAUTICS

WASHINGTON

July 15, 1955

CONFIDENTIAL

NATIONAL ADVISORY COMMITTEE FOR AERONAUTICS

RESEARCH MEMORANDUM

A DISCUSSION OF RECENT WIND-TUNNEL STUDIES RELATING  
TO THE PROBLEM OF ESTIMATING VERTICAL- AND  
HORIZONTAL-TAIL LOADS

By Richard E. Kuhn, Joseph M. Hallissy, Jr.,  
and Ralph W. Stone, Jr.

SUMMARY

Some of the effects of angle of attack, sideslip, Mach number, and airplane configuration on the vertical-tail loads and, to a lesser extent, horizontal-tail loads have been discussed. In addition, the division of load between the exposed vertical tail and the fuselage has also been considered. It has been shown that at low angles of attack, in both the subsonic and supersonic speed ranges, adequate predictions of the vertical-tail loads can be made. At angles of attack at which the flow begins to separate from the wing and fuselage, however, large rolled-up vortices appear in the flow in the region of the tail assembly and large changes in both vertical- and horizontal-tail loads result.

It has been shown that the effects of these vortices on the tail loads can be calculated if the strength and position of all vortices are known. For practical configurations with their complex fuselage shapes, however, it appears that, at present, some type of flow-visualization studies to indicate the vortex positions and some indication of the loads on the fuselage to estimate the vortex strength are necessary in order to estimate the tail loads.

INTRODUCTION

When an airplane is disturbed from equilibrium (as discussed in refs. 1 and 2), loads are developed on the tail surfaces of the airplane and usually act to oppose the motion of the airplane, that is, tend to bring the airplane back into equilibrium. The designer is interested in estimating these loads throughout the attitude range expected for the airplane in connection with both the stability of the configuration and the structural design of the tail surfaces themselves.

The present paper examines some recent wind-tunnel data on loads on vertical and horizontal tail surfaces of complete configurations in order

to point out some of the factors influencing the loads at high angles of attack. The data and discussion presented are limited to sideslip angles of the order of  $4^\circ$  or  $5^\circ$ .

## SYMBOLS

|          |  |
|----------|--|
| $C_N$    | normal-force coefficient, $N/qS_V$   |
| $C_B$    | bending-moment coefficient, $\frac{B}{q \frac{S_h}{2} \frac{b_h}{2}}$                        |
| $N$      | vertical-tail normal force, lb   |
| $B$      | root bending moment of horizontal-tail semispan, ft-lb                                       |
| $q$      | dynamic pressure, $\rho V^2/2$ , lb/sq ft  |
| $\rho$   | mass density, slugs/cu ft  |
| $V$      | free-stream velocity, ft/sec   |
| $M$      | Mach number  |
| $S_V$    | area of exposed vertical tail, sq ft   |
| $S_h$    | area of horizontal tail, sq ft   |
| $b_V$    | span of exposed vertical tail, ft  |
| $b_h$    | span of horizontal tail, ft  |
| $z$      | distance from fuselage-vertical-tail juncture to center of load on exposed vertical tail, ft |
| $L$      | lift on wing; or lift on fuselage alone, lb  |
| $l$      | effective span of wing; or effective diameter of fuselage, ft                                |
| $\Gamma$ | circulation, sq ft/sec   |
| $c_l$    | local section lift coefficient   |
| $c$      | local chord  |
| $c_{av}$ | average chord  |

## RESULTS AND DISCUSSION

## Vertical-Tail Loads at Low Angles of Attack

Procedures and data that can be used in estimating the loads on most tail configurations at both subsonic and supersonic speeds and at low angles of attack are available in the literature. References 3 to 13, for instance, present studies relating specifically to tail assemblies, and references such as 14 and 15, which relate to the lift-curve slope of lifting surfaces, can also be used provided the end-plate effect of the fuselage is properly accounted for. A comparison between the experimental and calculated vertical-tail normal-force coefficient at low angles of attack is presented in figure 1. The data presented were obtained by subtracting the measured side force on the model with the vertical tail removed from the measured side force on the complete model. Thus the results shown represent the total tail load which included both the normal force carried on the vertical tail and the additional increment of normal force that the vertical tail induced on the fuselage. The data were obtained from tests of the models at sideslip angles of the order of  $4^\circ$ .

In the supersonic speed range, the calculated variation, from reference 11, is in very good agreement with the experimental data which were obtained from an unpublished investigation. A rather complete discussion of the procedures for calculating the forces on the tail assembly of a complete configuration at supersonic speeds is included in reference 16.

References 14 and 17 were used for the calculations in the subsonic speed range. In making these calculations, the effective aspect ratio of the vertical tail was increased by the empirical relationship presented in reference 17 to account for the end-plate effect of the fuselage. The end-plate effect of the fuselage can also be treated by procedures such as those outlined in references 18 to 21. The experimental data shown at subsonic Mach numbers were obtained from reference 22. It should be remembered that the coefficients presented in the present paper are based on the exposed area of the vertical tail rather than on the area extended to the fuselage center line as is used in many of the references.

## Vertical-Tail Loads at High Angles of Attack

Experience has indicated that the methods of calculation used at low angles of attack do not hold throughout the angle-of-attack range because, at high angles of attack, the vertical tail is operating in the disturbed flow field from the wing and fuselage. Any attempt to calculate the tail loads at high angles of attack should be based on an understanding of the flow at the tail.

Flow field at tail.- At subsonic speeds, an idea of the nature of the flow at the location of the vertical tail can be obtained by means of the tuft-grid technique as discussed in references 23 and 24. The setup used in obtaining tuft-grid pictures is illustrated in figure 2. The tail surfaces are removed from the model and replaced by wires to indicate the location of the vertical tail and three possible horizontal-tail locations. The tuft grid is mounted immediately behind the model and is made of closely spaced vertical and horizontal wires with a tuft tied at each intersection. The camera views the tufts from a point on the axis of the tunnel far downstream of the model. If the flow is disturbed, as by a vortex trailing from a wing tip, the tufts will follow the local flow direction and a projection of the tuft will be seen. The orientation of the tuft will give an indication of the local sidewash and downwash.

A tuft-grid picture of the flow behind a model at an angle of attack of  $10^\circ$  and a sideslip angle of  $25^\circ$  is shown in figure 3. The model was painted black so as to make the tufts easier to see, and as a result the model itself is rather indistinct. The heavy white lines are the wires which indicate the location of the vertical tail and three possible horizontal-tail locations. The picture shows the system of vortices from the wing and fuselage. The fuselage vortex was found to originate at the nose of the fuselage.

In this case, a high sideslip angle was chosen so as to make the fuselage vortex more distinct. At smaller sideslip angles, the vortex would be less intense but would also be much closer to the vertical tail. Fuselage vortices have also been shown to exist at supersonic speeds, as shown in references 25 to 27. For these investigations the vapor-screen technique was used to obtain a picture of the flow.

The presence of these vortices at both subsonic and supersonic speeds is not surprising because their strength depends on the crossflow velocity (component of velocity perpendicular to the fuselage axis), and as long as the crossflow Mach number remains subcritical the strength of the vortices and their position would be expected to be relatively independent of Mach number effects.

The effect that a single vortex can have on the distribution of load on the vertical tail is illustrated in figure 4. Above the vortex, the sidewash from the vortex increases the local angles of attack on the vertical tail and thus increases the load. Below the vortex, the reverse is true, and the load is decreased.

Method of calculation.- Any procedure for estimating the effects that the vortices from the wing and fuselage have on the vertical-tail loads at high angles of attack should take into account the effects of all the vortices trailing from the wing and fuselage. It is necessary to know both the position and strength of each vortex.

The system used in this paper (fig. 5), although somewhat arbitrary, was deduced from inspection of tuft-grid and vapor-screen pictures and was selected from among the arrangements tried because it appeared to give reasonable agreement with experiment. It is presented here as an example of the type of vortex system which exists behind some configurations; however, it may not hold for all configurations.

A vortex from each wing was assumed to trail streamwise from the quarter-chord line of the wing. For the calculations in this paper, their lateral positions were judged by inspecting measured span load distributions on a wing of similar plan form. If vapor-screen or tuft-grid pictures of the flow behind the configuration in question are available, it would, of course, be preferable to use the positions indicated in these pictures. For the case of the wing vortices, tuft-grid or vapor-screen pictures at the Mach number in question will probably be necessary to locate accurately the vortices because the stall pattern on the wing and thus the positions of the vortices usually changes appreciably with Mach number. The strength of the vortices was determined from the vortex-lift equation

$$L = \rho V \Gamma l$$

where  $\Gamma$  is the vortex strength and  $l$  is the effective span of the wing over which the lift is assumed to be acting.

Two vortices were assumed to be shed by the fuselage and to be positioned as shown in figure 5. They were assumed to trail streamwise from the nose to the point of maximum fuselage cross-sectional area, from which point they were carried back parallel to the axis of the fuselage. This positioning was purely arbitrary but is seen to give reasonable agreement between calculated and measured vertical-tail loads for the configurations investigated. The radial positions of the vortices were determined by the orientation of the crossflow velocity, which is a function of both angle of attack and angle of sideslip, as shown in figure 5. The strength of the fuselage vortices was also determined on the basis of the above vortex-lift equation where, in this case,  $L$  is the combined components of the fuselage-alone lift and side force in the crossflow direction and the distance factor  $l$  was assumed to be the fuselage diameter.

For this paper, measured wing lift and measured lift and side-force data on the fuselage alone were used in computing the vortex strengths. Other papers which relate to the position and strength of vortices trailing from wing and fuselage shapes are listed as references 23 to 34.

Comparison of calculated and experimental total tail loads.- A comparison of the vertical-tail loads calculated by this procedure with measured loads for a high-wing and a low-wing model is shown in figure 6.

The data presented represent total tail loads as obtained from the difference between tail-on and tail-off tests. The agreement between the calculated and measured data indicates that these variations of total vertical-tail load apparently do result from a system of vortices similar to that assumed, although the strength and/or position of the vortices assumed for the high-wing configuration apparently were not exactly correct.

For these calculations, the effect of the vertical position of the wing on the sidewash at the vertical tail was accounted for by the procedure of reference 35. References 36 to 38 also give information relative to the effect of wing position on the sidewash at the vertical tail and thus on the tail loads.

As might be expected, the fuselage vortices were found to have the greatest effect on the vertical-tail loads. It would be expected, then, that the shape of the fuselage could also have a significant effect on the sidewash at the tail and thus on the tail loads.

The effect of fuselage shape on the vertical-tail loads is illustrated in figure 7. These data also represent the total tail load as obtained from the difference between tail-on and tail-off tests. Note the extreme variation of tail load for the square-fuselage configuration. This extreme variation is probably due to an appreciable increase in the strength of the vortices shed from the fuselage resulting from the square corners of the fuselage. The corners in this case were not sharp but had a radius of about 10 percent of the fuselage width. Lift data on the square fuselage alone were not available to use in estimating the strength of the fuselage vortices. It was necessary then to estimate the lift of the square fuselage, and this was done by increasing the viscous lift of the round fuselage by the ratio of the drag of a square rod to that of a round rod perpendicular to the wind. The positions of the vortices were assumed to be the same as those for the round fuselage.

The designer seldom has such simple fuselage shapes to deal with, however. A practical fuselage usually provides space and protuberances for such things as air intakes for the engines, radar domes, and the canopy for the pilot. The variation of total tail load with angle of attack for such a complex fuselage shape is also shown in figure 7. Fuselage-alone data were available for this configuration, but apparently there are other factors affecting the strength and/or position of the vortices at the intermediate angles of attack that were not considered.

The low value of vertical-tail load per degree of sideslip at high angles of attack, of course, does not necessarily indicate low overall tail loads because this low level also indicates that the configuration would have poor directional stability and under these conditions large sideslip angles might be expected. As a result, the tail loads at the high angles of attack may be more critical than at the lower angles of attack.

Division of load.- The data presented in figures 1, 6, and 7 represent the total vertical-tail load as determined from the difference between tail-on and tail-off tests and include both the load on the exposed part of the vertical tail and the load that the tail induces on the fuselage. These data are primarily of interest in connection with the stability of the airplane. For structural design the designer also would like to know the division of load between the fuselage and the exposed vertical tail. Recently two models have been instrumented with strain-gage balances in order to obtain some information on the breakdown in load between the exposed tail and the fuselage. One of these models is shown in figure 8. The strain-gage balance installed in the fuselage measured the load on the exposed part of the tail and the root bending moment about the dotted line. The model could be equipped with two alternate horizontal-tail configurations, one on the fuselage center line and one on top of the vertical tail in a T-configuration.

The division of load between the exposed tail and the fuselage for this model with the horizontal tail in the low position is shown in figure 9. The effect of relocating the horizontal tail from the low to the high position is shown in figure 10, and the effective position of the center of pressure of the load on the exposed vertical tail is presented in figure 11. This is referred to as an effective position of the center of pressure because it was obtained by dividing the measured root bending moment by the measured normal force, and, in the case of the high-horizontal-tail configuration, the measured root bending moment of the vertical tail included the rolling-moment couple that the horizontal tail imposes on the vertical tail. These data (figs. 9, 10, and 11) were obtained from tests at sideslip angles of  $\pm 4^\circ$ .

The calculated division of load between the exposed tail and the fuselage was obtained by calculating the span load distribution over the vertical tail by the procedure of reference 6 and integrating the loading over the appropriate part of the tail span. Contrary to the method of reference 6, wherein the entire fuselage load is estimated, the present paper deals only with the load induced on the fuselage by the vertical tail. The calculations were made, therefore, by assuming that the vertical tail was at an angle of incidence equal to the angle of sideslip and that the fuselage was at zero sideslip.

At the higher angles of attack the local angle-of-attack distribution over the vertical tail was modified by the sidewash from the system of vortices assumed (fig. 5) and the calculated load distribution was modified by a strip-theory analysis. The resulting modified load distribution (similar to fig. 4) was then integrated again over the appropriate percentage of tail span to obtain the division of load (fig. 9). The calculated center-of-pressure travel was also obtained from these calculations (fig. 11). Again the agreement is good, and in particular the calculated center-of-pressure variation indicates that the assumed vortex positions are approximately correct for this model.

Placing the horizontal tail atop the vertical tail (fig. 10) effectively increases the aspect ratio of the vertical tail and thus increases the load on the vertical tail. The estimated increment of vertical-tail load shown was obtained from reference 39 and was added to the angle-of-attack variation throughout the angle-of-attack range. Additional information on the effect of the horizontal tail, in any position, on the vertical-tail loads can be found in references 3, 4, 6 to 9, and 40.

The effect of Mach number in the transonic range on the division of load is illustrated in figure 12. The instrumentation of this model was similar to that for the model shown in figure 8. In general, the effects of Mach number are small, with the exception of the data for an angle of attack of  $13^\circ$ . References 14 and 17 were used in making the calculations shown. In making these calculations the effective aspect ratio of the vertical tail was increased (ref. 17) to account for the end-plate effect of the fuselage.

#### Horizontal-Tail Loads

Examination of tuft-grid pictures, such as figure 3, indicates that the horizontal tail can also be significantly affected by the system of vortices trailing from the wing and fuselage. In figure 3, the fuselage vortex is in a position to have serious effects on the load on a horizontal tail placed in the middle position. At higher angles of attack, the wing vortices can also have serious effects, because as the angle of attack is increased the wing tips begin to stall, and as the stall progresses the trailing vortices from the wing move in and approach the tail. If, in addition, the airplane is at an angle of sideslip, one tip of the tail moves toward the vortex. The effect that a single vortex can have on the load distribution on the horizontal tail is illustrated by the calculated load distributions in figure 13. The vortex has the greatest effect on the load distribution when it has moved inboard from the tip of the horizontal tail. Inboard of the vortex, the local angles of attack are decreased and the load is reduced. Outboard of the vortex the local angles and the load are increased.

Similar effects are shown in the experimental load distributions and root bending-moment coefficients shown in figure 14. The measured load distributions were obtained with the horizontal tail set at zero incidence. Note the rapid increase in the difference between the root bending-moment coefficient of the right and left semispans of the horizontal tail at the highest angles of attack ( $M = 0.8$ ). This trend is apparently due to the effects of the trailing vortex from the right wing as shown by the measured span load distribution.

At a Mach number of 0.98 these large changes in load are apparently not present in the angle-of-attack range tested, because at this Mach

number the stall pattern of the wing has changed and the trailing vortices from the wing have not moved in. References 31, 32, 41, and 42 also deal with the problem of asymmetric loads on the horizontal tail or the effects of trailing vortices. There are other factors, such as the fuselage vortices and the load that the vertical tail induces on the horizontal tail, that are affecting the measured load distribution shown in figure 14. These factors were not considered in the calculated load distributions shown in figure 13.

#### CONCLUDING REMARKS

Some of the effects of angle of attack, sideslip, Mach number, and airplane configuration on the vertical-tail loads and, to a lesser extent, horizontal-tail loads have been discussed. In addition, the division of load between the exposed vertical tail and the fuselage has also been considered. It has been shown that at low angles of attack, in both the subsonic and supersonic speed ranges, adequate predictions of the vertical-tail loads can be made. At angles of attack at which the flow begins to separate from the wing and fuselage, however, large rolled-up vortices appear in the flow in the region of the tail assembly and large changes in both vertical- and horizontal-tail loads result.

It has been shown that the effects of these vortices on the tail loads can be calculated if the strength and position of all vortices are known. For practical configurations with their complex fuselage shapes, however, it appears that, at present, some type of flow-visualization studies to indicate the vortex positions and some indication of the loads on the fuselage to estimate the vortex strength are necessary in order to estimate the tail loads.

Langley Aeronautical Laboratory,  
National Advisory Committee for Aeronautics,  
Langley Field, Va., April 22, 1955.

## REFERENCES

1. Zimmerman, Charles H.: Recent Stability and Aerodynamic Problems and Their Implications as to Load Estimation. NACA RM L55E11a, 1955.
2. Weil, Joseph, Gates, Ordway B., Jr., Banner, Richard D., and Kuhl, Albert E.: Flight Experience of Inertia Coupling in Rolling Maneuvers. NACA RM H55E17b, 1955.
3. Queijo, M. J., and Riley, Donald R.: Calculated Subsonic Span Loads and Resulting Stability Derivatives of Unswept and  $45^\circ$  Sweptback Tail Surfaces in Sideslip and in Steady Roll. NACA TN 3245, 1954.
4. Riley, Donald R.: Effect of Horizontal-Tail Span and Vertical Location on the Aerodynamic Characteristics of an Unswept Tail Assembly in Sideslip. NACA Rep. 1171, 1954. (Supersedes NACA TN 2907.)
5. Lyons, D. J., and Bisgood, P. L.: An Analysis of the Lift Slope of Aerofoils of Small Aspect Ratio, Including Fins, With Design Charts for Aerofoils and Control Surfaces. R. & M. No. 2308, British A.R.C., 1945.
6. Wiley, Harleth G., and Riley, Donald R.: An Experimental and Theoretical Investigation at High Subsonic Speeds of the Effects of Horizontal-Tail Height on the Aerodynamic Characteristics in Sideslip of an Unswept, Untapered Tail Assembly. NACA RM L53J19, 1953.
7. Wiley, Harleth G., and Moseley, William C., Jr.: An Investigation at High Subsonic Speeds of the Pressure Distributions on a  $45^\circ$  Sweptback Vertical Tail in Sideslip With and Without a  $45^\circ$  Sweptback Horizontal Tail Located on the Fuselage Center Line. NACA RM L54H23, 1954.
8. Wiley, Harleth G., and Moseley, William C., Jr.: Investigation at High Subsonic Speeds of the Pressure Distribution on a  $45^\circ$  Sweptback Vertical Tail in Sideslip With a  $45^\circ$  Sweptback Horizontal Tail Mounted at 50-Percent and 100-Percent Vertical-Tail Span. NACA RM L54I08, 1954.
9. Wiley, Harleth G., and Moseley, William C., Jr.: An Investigation at High Subsonic Speeds of the Effects of Horizontal-Tail Height on the Aerodynamic and Loading Characteristics in Sideslip on a  $45^\circ$  Sweptback, Untapered Tail Assembly As Determined From Force Tests and Integrated Vertical-Tail Span Loadings. NACA RM L55E04, 1955.
10. Bobbitt, Percy J.: Theoretical Calculations of the Lateral Stability Derivatives for Triangular Vertical Tails With Subsonic Leading Edges Traveling at Supersonic Speeds. NACA TN 3240, 1954.

11. Martin, John C., and Malvestuto, Frank S., Jr.: Theoretical Force and Moments Due to Sideslip of a Number of Vertical Tail Configurations at Supersonic Speeds. NACA TN 2412, 1951.
12. Malvestuto, Frank S., Jr.: Theoretical Supersonic Force and Moment Coefficients on a Sideslipping Vertical- and Horizontal-Tail Combination With Subsonic Leading Edges and Supersonic Trailing Edges. NACA TN 3071, 1954.
13. Margolis, Kenneth: Theoretical Calculations of the Pressures, Forces, and Moments Due to Various Lateral Motions Acting on Thin Isolated Vertical Tails With Supersonic Leading and Trailing Edges. NACA TN 3373, 1955.
14. DeYoung, John, and Harper, Charles W.: Theoretical Symmetric Span Loading at Subsonic Speeds for Wings Having Arbitrary Plan Form. NACA Rep. 921, 1948.
15. Polhamus, Edward C.: A Simple Method of Estimating the Subsonic Lift and Damping in Roll of Sweptback Wings. NACA TN 1862, 1949.
16. Margolis, Kenneth, and Bobbitt, Percy J.: Theoretical Calculations of the Stability Derivatives at Supersonic Speeds for a High-Speed Airplane Configuration. NACA RM L53G17, 1953.
17. Queijo, M. J., and Wolhart, Walter D.: Experimental Investigation of the Effect of Vertical-Tail Size and Length and of Fuselage Shape and Length on the Static Lateral Stability Characteristics of a Model with  $45^\circ$  Sweptback Wing and Tail Surfaces. NACA Rep. 1049, 1951. (Supersedes NACA TN 2168.)
18. Michael, William H., Jr.: Investigation of Mutual Interference Effects of Several Vertical-Tail-Fuselage Configurations in Sideslip. NACA TN 3135, 1954.
19. Zlotnick, Martin, and Robinson, Samuel W., Jr.: A Simplified Mathematical Model for Calculating Aerodynamic Loading and Downwash for Wing-Fuselage Combinations With Wings of Arbitrary Plan Form. NACA TN 3057, 1954. (Supersedes NACA RM L52J27a.)
20. Robinson, Samuel W., Jr., and Zlotnick, Martin: A Method for Calculating the Aerodynamic Loading on Wing-Tip-Tank Combinations in Subsonic Flow. NACA RM L53B18, 1953.
21. Lawrence, H. R., and Flax, A. H.: Wing-Body Interference at Subsonic and Supersonic Speeds - Survey and New Developments. Jour. Aero. Sci., vol. 21, no. 5, May 1954, pp. 289-324.

22. Kuhn, Richard E., and Wiggins, James W.: Static Lateral Stability Characteristics of a  $\frac{1}{10}$  - Scale Model of the X-1 Airplane at High Subsonic Mach Numbers. NACA RM L51F01a, 1951.
23. Bird, John D., and Riley, Donald R.: Some Experiments on Visualization of Flow Fields Behind Low-Aspect-Ratio Wings by Means of a Tuft Grid. NACA TN 2674, 1952.
24. Michael, William H., Jr.: Flow Studies in the Vicinity of a Modified Flat-Plate Rectangular Wing of Aspect Ratio 0.25. NACA TN 2790, 1952.
25. Seiff, Alvin, Sandahl, Carl A., Chapman, Dean R., Perkins, E. W., and Gowen, F. E.: Aerodynamic Characteristics of Bodies at Supersonic Speeds. A Collection of Three Papers. NACA RM A51J25, 1951.
26. Perkins, Edward W., and Kuehn, Donald M.: Comparison of the Experimental and Theoretical Distributions of Lift on a Slender Inclined Body of Revolution at  $M = 2$ . NACA RM A53E01, 1953.
27. Allen, H. Julian, and Perkins, Edward W.: Characteristics of Flow Over Inclined Bodies of Revolution. NACA RM A50L07, 1951.
28. Bollay, William: A Non-Linear Wing Theory and Its Application to Rectangular Wings of Small Aspect Ratio. Z.f.a.M.M., Bd. 19, Nr. 1, Feb. 1939, pp. 21-35.
29. Brown, Clinton E., and Michael, William H., Jr.: On Slender Delta Wings With Leading-Edge Separation. NACA TN 3430, 1955.
30. Spreiter, John R.: Downwash and Sidewash Fields Behind Cruciform Wings. NACA RM A51L17, 1952.
31. Rogers, Arthur W.: Application of Two-Dimensional Vortex Theory to the Prediction of Flow Fields Behind Wings of Wing-Body Combinations at Subsonic and Supersonic Speeds. NACA TN 3227, 1954.
32. Lomax, Harvard, and Byrd, Paul F.: Theoretical Aerodynamic Characteristics of a Family of Slender Wing-Tail-Body Combinations. NACA TN 2554, 1951.
33. Landahl, Mårten T.: Analysis of Some Wing-Body-Vertical Tail Interference Problems for Non-Symmetric Steady Flow Using Slender-Body Theory. KTH-Aero TN 32, Roy. Inst. of Tech., Div. of Aero. (Stockholm, Sweden), 1953.

34. Spahr, J. Richard: Longitudinal Aerodynamic Characteristics to Large Angles of Attack of a Cruciform Missile Configuration at a Mach Number of 2. NACA RM A54H27, 1954.
35. Goodman, Alex, and Thomas, David F., Jr.: Effects of Wing Position and Fuselage Size on the Low-Speed Static and Rolling Stability Characteristics of a Delta-Wing Model. NACA TN 3063, 1954.
36. Multhopp, H.: Aerodynamics of the Fuselage. NACA TM 1036, 1942.
37. House, Rufus O., and Wallace, Arthur R.: Wind-Tunnel Investigation of Effect of Interference on Lateral-Stability Characteristics of Four NACA 23012 Wings, an Elliptical and a Circular Fuselage, and Vertical Fins. NACA Rep. 705, 1941.
38. Goodman, Alex: Effects of Wing Position and Horizontal-Tail Position on the Static Stability Characteristics of Models With Unswept and  $45^\circ$  Sweptback Surfaces With Some Reference to Mutual Interference. NACA TN 2504, 1951.
39. Brewer, Jack D., and Lichtenstein, Jacob H.: Effect of Horizontal Tail on Low-Speed Static Lateral Stability Characteristics of a Model Having  $45^\circ$  Sweptback Wing and Tail Surfaces. NACA TN 2010, 1950.
40. Katzoff, S., and Mutterperl, William: The End-Plate Effect of a Horizontal-Tail Surface on a Vertical-Tail Surface. NACA TN 797, 1941.
41. Braun, Winfried: Asymmetric Tailplane Loads Due to Sideslip. Tech. Note No. Structures 81, British R.A.E., Jan. 1952.
42. Cooney, T. V.: The Unsymmetrical Load and Bending Moment on the Horizontal Tail on a Jet-Powered Bomber Measured in Sideslipping Flight. NACA RM L51J24, 1952.

TOTAL VERTICAL-TAIL LOADS AT SMALL ANGLES OF ATTACK

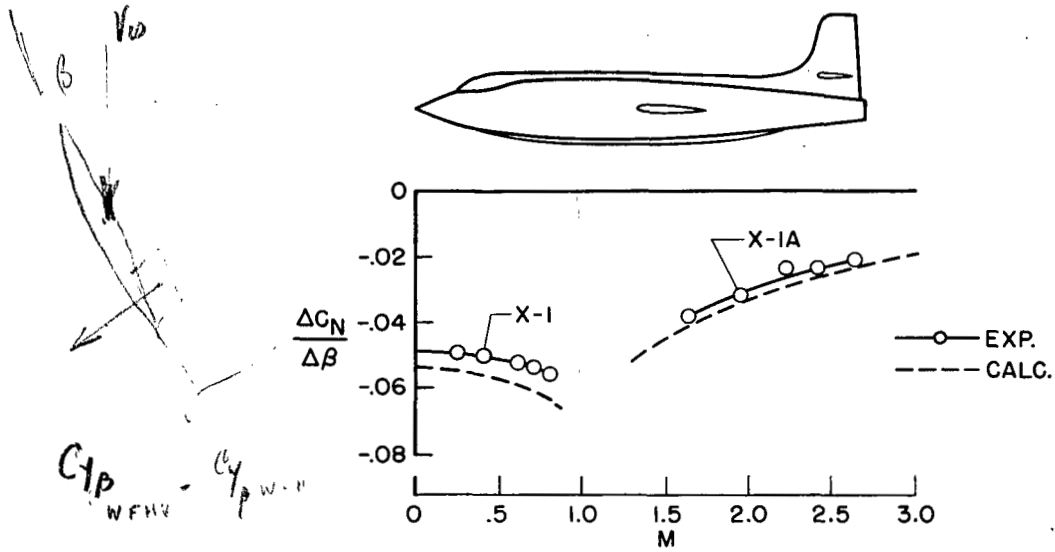


Figure 1

SETUP FOR FLOW SURVEY WITH TUFT GRID

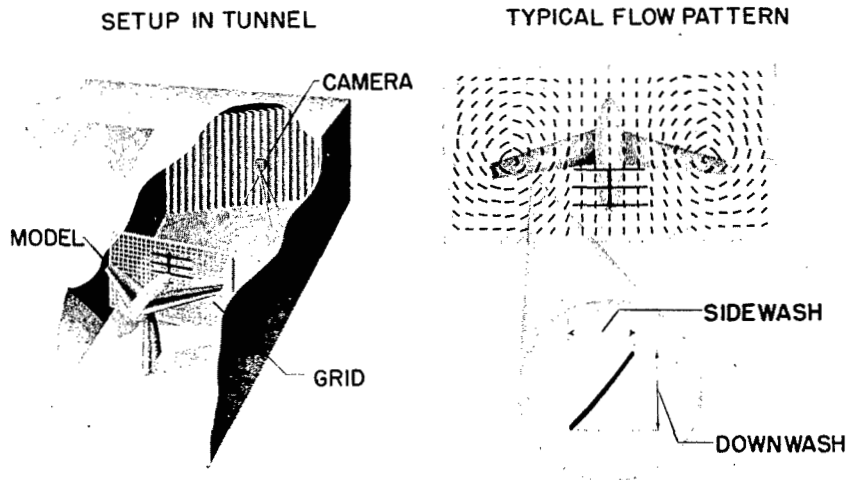


Figure 2

FLOW FIELD BEHIND MODEL  
 $\alpha = 10^\circ$ ;  $\beta = 25^\circ$

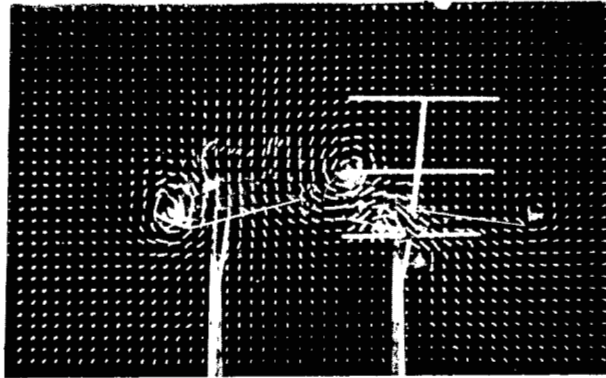


Figure 3

EFFECT OF FUSELAGE VORTEX ON VERTICAL-TAIL  
LOAD DISTRIBUTION

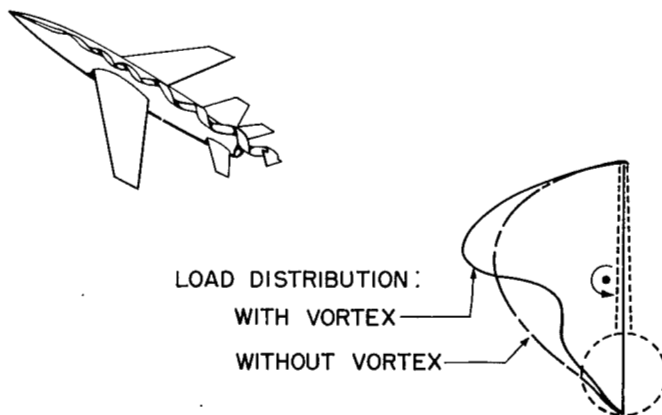


Figure 4

VORTEX SYSTEM USED TO APPROXIMATE THE FLOW FIELD

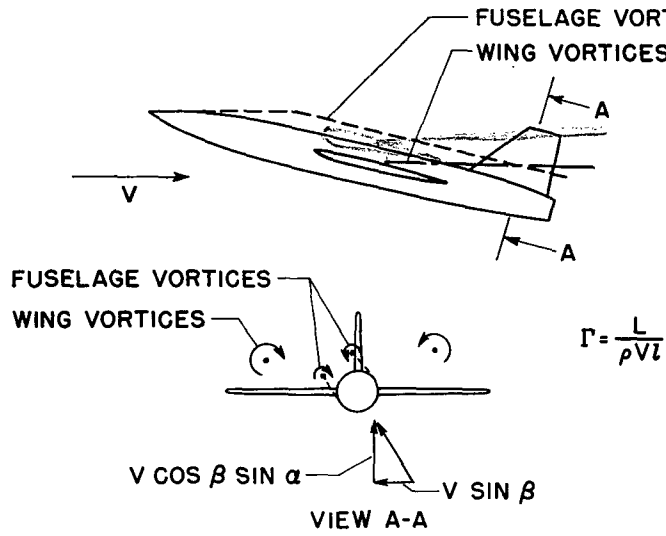


Figure 5

EFFECT OF WING HEIGHT ON TOTAL VERTICAL-TAIL LOAD  
M=0.8

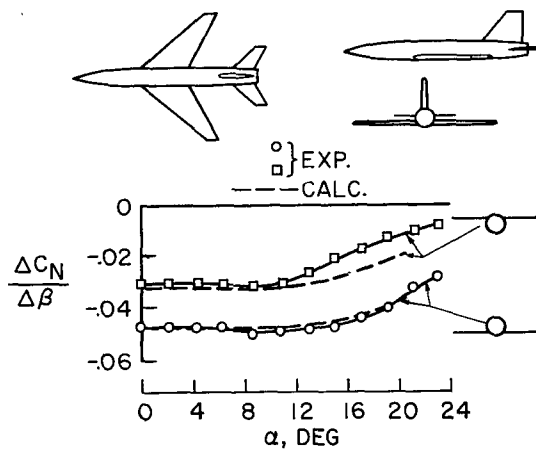


Figure 6

EFFECT OF FUSELAGE SHAPE  
M = 0.8

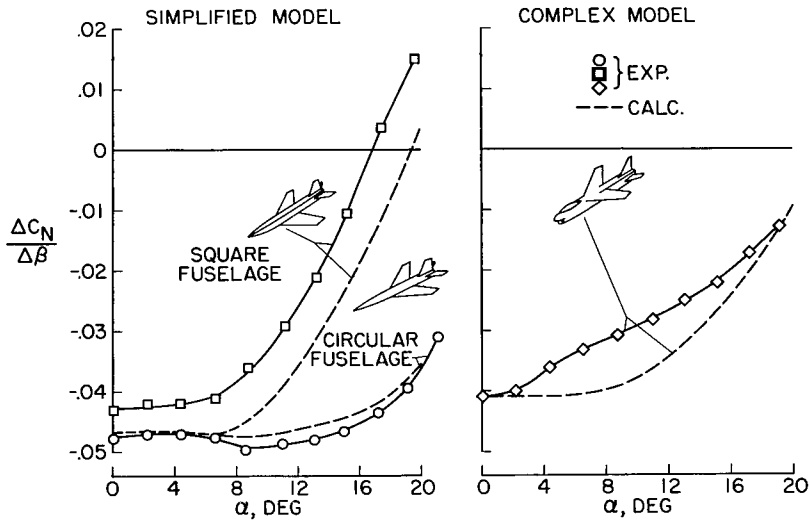


Figure 7

MODEL USED IN INVESTIGATIONS OF  
LOAD ON EXPOSED VERTICAL TAIL

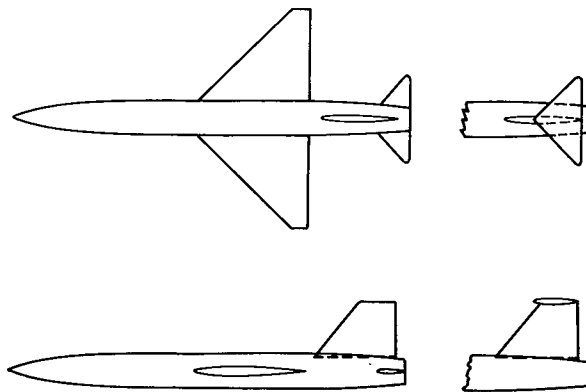


Figure 8

COMPARISON OF TOTAL VERTICAL-TAIL  
LOAD AND LOAD ON EXPOSED TAIL  
M=0.80; LOW HORIZONTAL TAIL

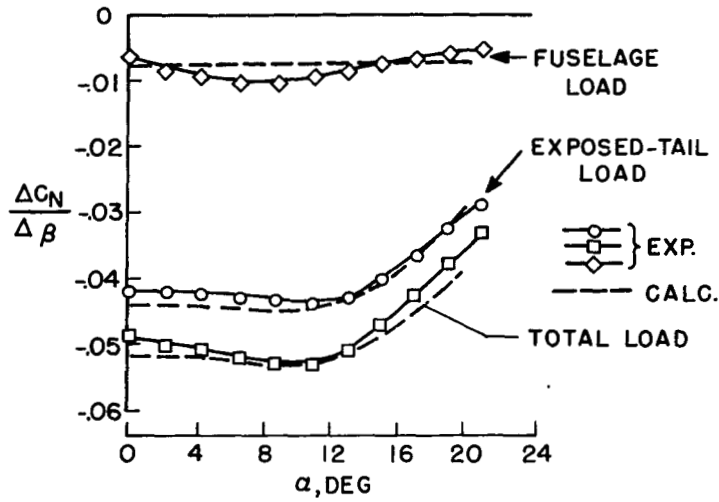


Figure 9

EFFECT OF HORIZONTAL-TAIL POSITION  
ON EXPOSED-VERTICAL-TAIL LOAD  
M=0.8

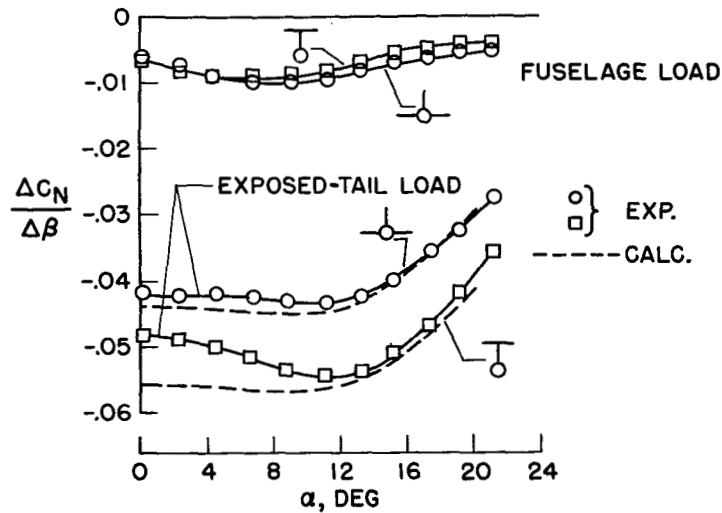


Figure 10

EFFECTIVE SPANWISE POSITION OF LOAD ON EXPOSED TAIL

M=0.80

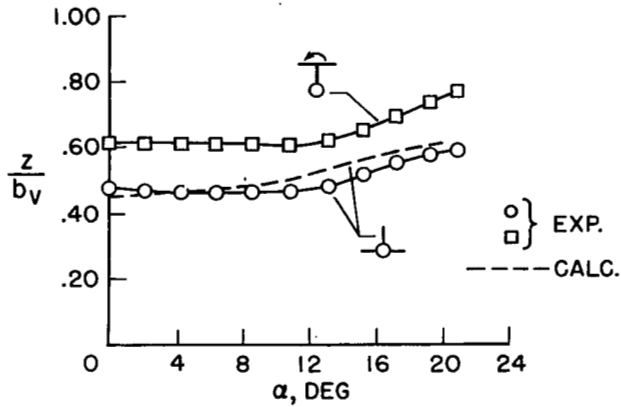


Figure 11

EFFECT OF MACH NUMBER ON TAIL LOAD

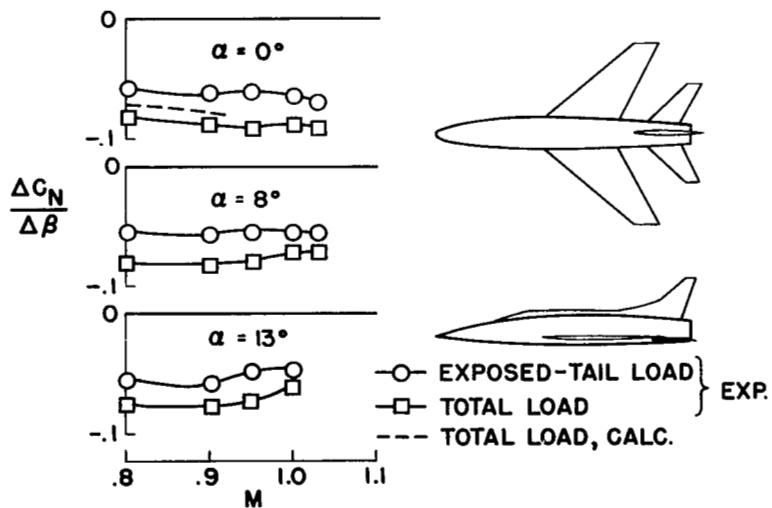


Figure 12

WING-VORTEX EFFECT ON HORIZONTAL-TAIL  
LOAD DISTRIBUTION  
CONSTANT TOTAL LOAD

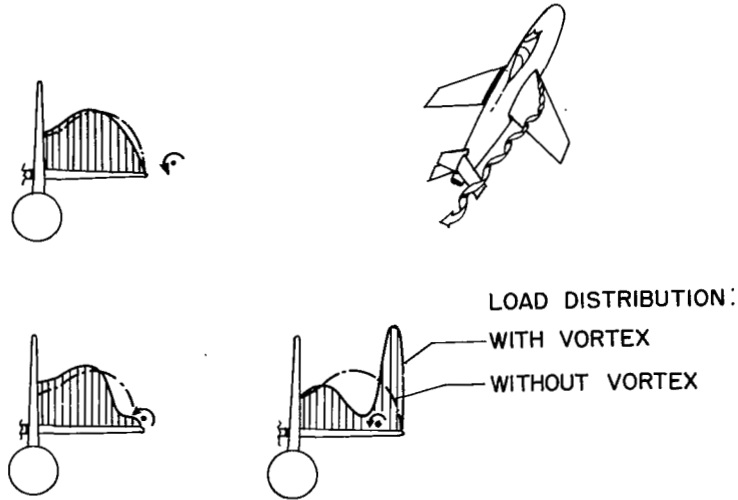


Figure 13

HORIZONTAL-TAIL LOADS IN SIDESLIP  
 $\beta = 5^\circ$

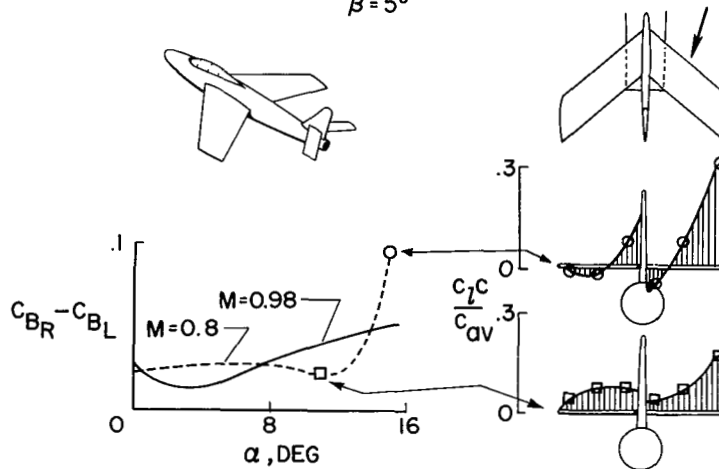


Figure 14